Embryonic tissues are viscoelastic materials

D.A. Beysens, G. Forgacs, and J.A. Glazier

Abstract: Early embryonic development is characterized by spectacular morphogenetic processes such as sorting or spreading of tissues. Analogy between viscoelastic fluids and certain properties of embryonic tissues turned out to be useful in interpreting some aspects of these morphogenetic phenomena. In accordance with the differential adhesion hypothesis, the values of tissue-specific surface tensions have been shown to be consistent with the equilibrium configurations such tissues reach in the course of sorting and spreading. A method to measure tissue surface tension and viscoelastic properties is described. Notions like the Laplace's equation relating surface tension to radii of curvature, or the Kelvin model of viscoelasticity are used to analyze the results of these measurements. The fluid analogy is extended to time-dependent phenomena, in particular, to the analysis of cellular pattern evolution in the course of spreading. On the basis of recent experimental findings, we demonstrate that the kinetics of spreading and nucleation in binary fluids can be analyzed using the same formalism. We illustrate how our results can be used to obtain biologically relevant information on the strength of binding between specific cell adhesion molecules under near physiological conditions. We also suggest a diagnostic application of our method to monitor the metastatic potential of tumors.

PACS No.: 03.65Ge

Résumé: Au début, le développement embryonnaire se caractérise par des mécanismes morphogéniques spectaculaires, comme la différentiation et la multiplication des tissus. Il est utile d'établir une analogie entre les fluides viscoélastiques et des propriétés des tissus embryonnaires afin de mieux interpréter certains aspects de ces phénomènes morphogéniques. En accord avec l'Hypothèse d'Adhésion Différentielle, on montre que les valeurs de tension de surface des tissus sont cohérentes avec les configurations à l'équilibre que ces tissus atteignent dans le cours de la différentiation et de l'expansion. Nous décrivons une méthode pour mesurer la tension de surface des tissus et les propriétés viscoélastiques des fluides. Dans l'analyse de ces mesures, nous utilisons l'équation de Laplace qui relie la tension de surface au rayon de courbure ou le modèle de Kelvin pour la viscoélasticité. Nous étendons l'analogie avec le liquide aux phénomènes dépendant du temps, en particulier l'évolution du patron cellulaire lors de la multiplication. Sur la base de récents résultats expérimentaux, nous montrons que la cinétique de différentiation et de nucléation dans les fluides binaires peut être analysée à l'aide du même formalisme. Nous montrons comment nos résultats permettent d'obtenir de l'information biologiquement significative sur la force du lien entre les molécules d'ahésion cellulaire dans des conditions proches des conditions qui sont proches des conditions physiologiques. Nous suggérons une utilisation diagnostique de notre méthode pour étudier le potentiel métastatique des tumeurs.
[Traduit par la rédaction]

Received October 10, 1999. Accepted April 12, 2000. Published on the NRC Research Press Web site on June 23, 2000.

D.A. Beysens. Département de Recherche Fondamentale sur la Matière Condensée, CEA Grenoble, 38054 Grenoble, France.
G. Forgacs.[1] Department of Physics and Biology, Clarkson University, Potsdam, NY 13699-5820, U.S.A.
J.A. Glazier. Department of Physics, University of Notre-Dame, Notre-Dame, IN 46556, U.S.A.

[1] Corresponding author: **e-mail:** forgacs@clarkson.edu

1. Introduction

Tissues and cells contain complex subunits and have a variety of functions controlled by intricately coupled genetic and chemical pathways. In spite of the plethora of such pathways, a simple analogy between the behavior of tissues and fluids explains a number of early developmental phenomena [1,2]. Typical such phenomena are spreading and cell sorting. During embryonic morphogenesis, it is common for one cell population to spread over the surface of another, just as coalescing droplets of immiscible liquids do. When cells of tissues that are neighbors in normal development are dissociated into single cells and then randomly intermixed, they reorder themselves to recover their physiological configuration [3]. In particular, in an initially random mixture of endodermal and ectodermal *Hydra* cells, the endodermal cells sort to the center of the aggregate and the ectodermal cells surround them. Eventually, the entire organism regenerates [4]. Sorting is not limited to tissues that encounter each other in normal development: it takes place between any pair of tissues, provided that one is more cohesive than the other [5].

To account for the fluidlike behavior of cell populations that display it, Steinberg formulated the "differential adhesion hypothesis" (DAH) [2,6–10]. According to the DAH, the behavior of cell populations in spreading and sorting, like that of ordinary liquids, is due to their possession of surface and interfacial tensions, generated by adhesive and cohesive interactions between the component subunits (molecules in the one case, cells in the other). Recent experimental results have demonstrated that (*i*) tissue surface tension is a well-defined intensive physical parameter that characterizes the equilibrium shape of certain multicellular aggregates and (*ii*) the measured values of these tensions account for the observed mutual envelopment behavior of the corresponding tissues [11]. Computer simulations applying the principles of the DAH and utilizing specific statistical mechanical models reproduce the equilibrium configurations that tissues attain in the course of sorting experiments [12,13]. Recent in vivo experiments have confirmed DAH [14,15].

Surface tension is an equilibrium property. Even if differences in surface tension contribute to the driving force for movement during morphogenesis, by themselves they reveal little about the time course of such processes. The kinetics of cell sorting and tissue envelopment depends upon the dynamical properties of cell populations. Early experiments by Phillips and coworkers [16,17] showed that embryonic cell aggregates behave like deformable solids during brief experimental manipulations, but like viscous liquids in long-term organ cultures; that is, they possess complex viscoelastic characteristics. This is not surprising, considering that major components of individual cells themselves display viscoelastic properties. The viscoelastic moduli of the cytoplasm of various cells have been measured [18–23]. Detailed experiments on the viscoelasticity of solutions of major cytoplasmic biopolymers like microtubules, actin microfilaments, and intermediate filaments have been used to suggest possible specialized roles for the different classes of filaments in vivo [24–27]. Following the deformations of red blood cells, Engelhardt and Sackmann [28] were able to deduce values for the shear elastic moduli and viscosities of erythrocyte plasma membranes.

Despite the fact that much information exists on the viscoelastic properties of various cellular components [26], relatively little effort has been devoted to rheological studies of living tissues [29]. Gordon et al. [30] estimated the viscosity of several embryonic chicken-cell populations, but the applied method gave no information on viscoelasticity. Recently, using a specifically designed apparatus, Forgacs et al. [31] were able to measure the viscoelastic properties of a number of embryonic tissues.

In the present work we demonstrate that the analogy between fluids or viscoelastic materials and embryonic tissues (*i*) can be extended to time-dependent phenomena, namely, the kinetics of sorting and (*ii*) allows us to deduce biologically relevant information on cell adhesion.

The paper is organized as follows. First, we describe a method to measure tissue viscoelasticity and demonstrate how to analyze such measurements in terms of tissue-specific physical properties. We show that when a cell aggregate is subject to external forces it relaxes to an equilibrium shape consistent with the minimum of its interfacial free energy (the interface being formed between the aggregate and

Fig. 1. Schematic representation of the compression plate apparatus. For symbols, see text.

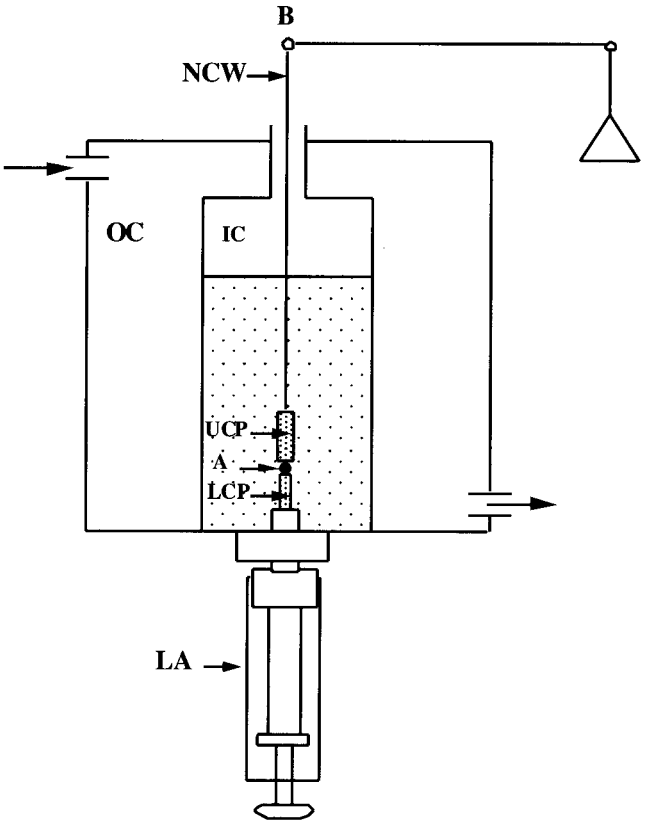

the surrounding tissue culture medium). In the course of the relaxation process, the aggregate shows a behavior typical for viscoelastic materials. Next, we report some recent experimental results on the kinetics of cell sorting and analyze them using the fluid analogy of tissues and DAH. Finally, we conclude with a discussion on the biological implications of our findings.

2. A method to measure tissue viscoelasticity

To study the viscoelastic properties of living tissues, we prepare spherical cell aggregates from various chicken embryonic tissues. We dissect the eyes, heart, and liver using sterile techniques [32]. We dissociate the tissues into individual cells using Trypsin-EDTA (to temporarily inactivate cell adhesion), incubate the cells in a culture medium, and then centrifuge them to obtain thin pellets. These pellets are cut into fragments, 0.6–1 mm in diameter, containing 30–40 thousand cells. The fragments are placed in a gyratory shaker for 10–12 h, depending on the tissue type, by which time they round up and form spherical aggregates with a diameter of 200–500 μm. The fact that these aggregates round up and minimize their surface area with the surrounding tissue culture medium is a further manifestation of the liquidlike character of their equilibrium configurations. Figure 1 shows a specifically designed apparatus that we use to measure the viscoelastic properties of cell aggregates or model tissues. The apparatus consists of an inner (IC) and outer chamber (OC), which are separated by a glass wall. The OC is used for circulating water at 37°C (provided by a circulating water bath), to maintain the physiological

Fig. 2. A characteristic compression force relaxation for a chicken embryonic heart aggregate. Dots denote experimental values, the continuous line is the fit based on the Kelvin model discussed in the text.

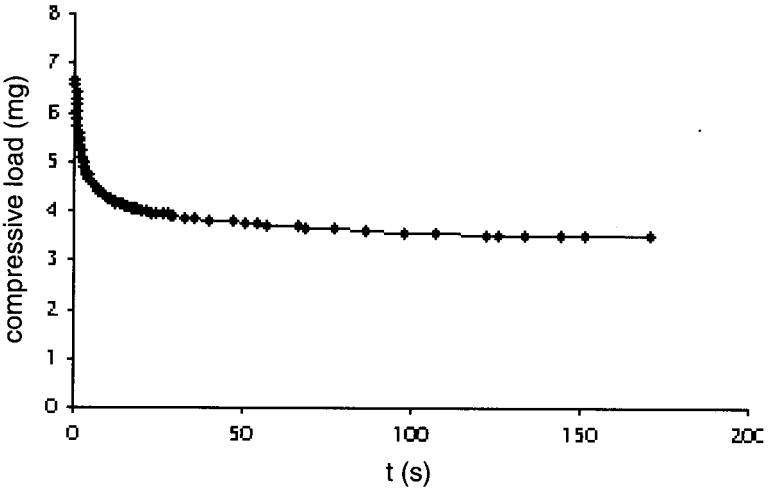

Fig. 3. Definition of the quantities used in expression (1). R_1 and R_2 are the two principal radii of curvature, at the droplet's equator and in a plane through the axis of symmetry. R is the radius of the droplet's circular area of contact with the plates.

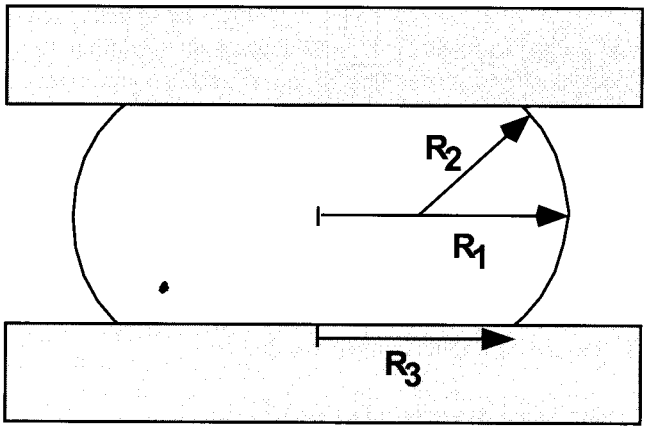

temperature in the IC, which contains living cells. The IC is filled with a tissue culture medium, the necessary medium to keep cells healthy during the experimental manipulations. A spherical aggregate (A) is compressed and then let to relax between the lower (LCP) and the upper (UCP) compression plates, by turning the lower assembly (LA). The plates are coated with poly(2-hydroxyethylmethacrylate) or poly(HEMA) [33] to minimize their adherence to the cell aggregate. The UCP hangs from the arm of an electrobalance (through a nickel–chromium wire, NCW). The shape of the aggregate in the course of the relaxation process is monitored through a horizontally positioned microscope and is recorded by two video cameras (positioned at 90° angles relative to each other) attached to a time-lapse video recorder. The video recorder is attached to a computer, which is equipped with a National Instrument I/O card and Labview software for data acquisition and a composite color PCI frame grabber.

Fig. 4. Schematic illustration of the Kelvin model of viscoelasticity used in this work. For the definition of symbols, see text.

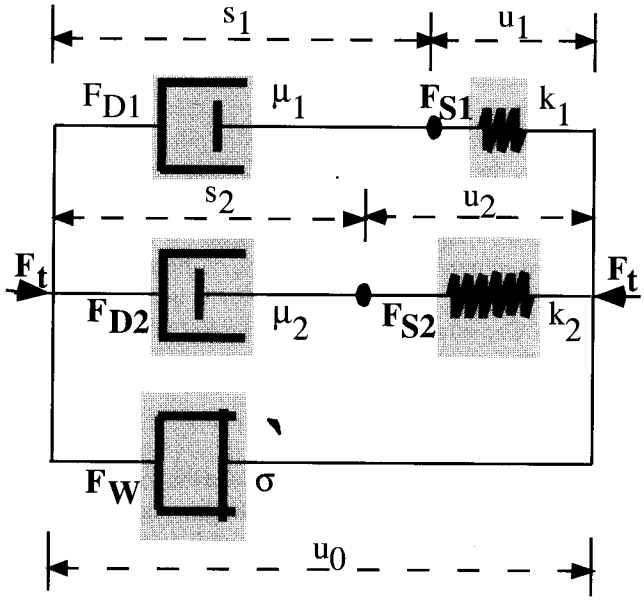

3. Tissue surface tension

The equilibrium value of the compressive force F_{eq} (see Fig. 2) and the shape of the compressed aggregate determine the surface tension σ (i.e., the interfacial tension between the tissue and the surrounding tissue culture medium) through Laplace's equation [34]

$$\frac{F_{eq}}{\pi R_3^2} = \sigma\left(\frac{1}{R_1} + \frac{1}{R_2}\right) \tag{1}$$

In (1) R_1 and R_2 are the principal radii of curvature as shown in Fig. 3 and πR_3^2 measures the area of contact between the cell aggregate and either of the parallel compression plates. Relaxation curves similar to the one shown in Fig. 2 were obtained for multicellular aggregates derived from five embryonic chicken tissues: neural retina, liver, heart ventricle, pigmented epithelium, and limb bud mesoderm. To verify that the determined values of the surface tension corresponded to a true intensive thermodynamic quantity, we repeated the measurements varying the aggregate size and the magnitude of the initial compressive force. Within our accuracy σ was insensitive to these modifications. The measured values of tensions for the five chicken embryonic tissues varied from 1.6 (neural retina) to 20 (limb bud) dyn/cm (1 dyn = 10^{-5} N) [11].

Surface tension, which in the case of liquids is identical to the surface free energy per unit area, contains information on the cohesion of the subunits forming the system in question (i.e., cells for tissues). Indeed, simple dimensional analysis reveals that $\sigma \propto NJ$, where N is the number of bound cell-adhesion molecules per unit surface of a cell and J is the effective binding energy of a pair of such molecules on two neighboring adhering cells.

4. Tissue viscoelasticty

The relaxation curve shown in Fig. 2 is typical for viscoelastic materials: it shows a bimodal process. An initial rapid elastic response is followed by a slower viscous response. To fully analyze such curves a specific model of viscoelasticity has to be adopted. A generalized Kelvin model [29], illustrated in Fig. 4, accurately fits the data, as can be seen in Fig. 2. The two dashpots (with friction constants μ_1 and μ_2) and two springs (with spring constants k_1 and k_2) represent the simplest viscoelastic circuit to describe the bimodal relaxation process. As discussed earlier, the equilibrium shape of the aggregate is determined by its surface tension, as modeled by the slidewire element (with surface tension σ). Details of this model have been given in ref. 31. The initial sudden compression produces an instantaneous deformation of the slidewire element, u_0 and of the two springs, u_1 and u_2, whereas the initial displacement of the dashpots ($s_1(0)$ and $s_2(0)$) is zero. The total compressive force F_t acting on the aggregate is $F_t = F_{S_1} + F_{S_2} + F_W = F_{D_1} + F_{D_2} + F_W$, where $F_{S_{1,2}}$, $F_{D_{1,2}}$, and F_W are the forces acting on the springs, dashpots, and slidewire element, respectively. The total deformation of the Kelvin body, which corresponds to F_t is $u_t = u_1 + s_1 = u_2 + s_2 = u_0$. The relationship between forces and deformations is

$$F_{S_1}(t) = k_1 u_1(t) = F_{D_1}(t) = \mu_1 \dot{s}_1(t), \quad F_{S_2}(t) = k_2 u_2(t) = F_{D_2}(t) = \mu_2 \dot{s}_2(t), \quad F_W(t) = \sigma u_0(t) \quad (2)$$

Here, the dots denote differentiation with respect to time. Since the overall shape of the aggregate is not changing during force relaxation, we have $u_t = u_0 = \text{const}$. This implies that $F_W = F_{eq}$, where F_{eq} is given by (1). Finally, the equation governing the relaxation of F_t takes the form

$$F_t + \left(\frac{\mu_1}{k_1} + \frac{\mu_2}{k_2}\right)\dot{F}_t + \frac{\mu_1 \mu_2}{k_1 k_2}\ddot{F}_t = \sigma u_0 \quad (3)$$

The solution of (3) is

$$F_t(t) = \left(\sigma + k_1 \mathrm{e}^{-t/\tau_1} + k_2 \mathrm{e}^{-t/\tau_2}\right)u_0 \quad (4)$$

Here the two relaxation times are given by

$$\tau_i = \frac{\mu_i}{k_i}, \qquad i = 1, 2 \quad (5)$$

Fitting the expression in (4) to the measured relaxation curves (see Fig. 2) determines τ_1 and τ_2, along with the viscoelastic parameters k_1, k_2, μ_1, and μ_2. We have found that τ_1 and τ_2 differ at least by one order of magnitude for all the five tissues, showing the clear separation of the elastic and viscous contributions to the relaxation [31].

Upon compression between the parallel plates the originally spherical aggregate becomes doughnut shaped (see Fig. 3). Moreover, as earlier studies by Phillips and co-workers revealed [16,35], the shape of the individual cells within the aggregates changes from the precompressed cuboidal to a compressed elongated, and finally returns to the cuboidal. In other words, the initial stress causing the shape deformation is fully dissipated from the interior of the aggregate by the time the aggregate reaches equilibrium. Any stress left in the system must therefore reside in its surface layer. Since the overall surface area of the compressed aggregate is larger than its precompressed area, this finding implies that some interior cells must have moved to the surface. Such movement is hindered by the friction between cells, which is characterized by μ_2, the friction constant relevant for the later more viscous phase of the relaxation process. (Note that in the initial more elastic phase cells do not move.) The stronger cells adhere (i.e., the larger is J), the larger is μ_2. The more adhesion bonds connect neighboring cells (i.e., the larger is N), the larger is μ_2. The longer these bonds survive, again the larger is μ_2. Finally, $\mu_2 \propto NJ\tau$, where τ is the characteristic lifetime of an adhesion pair. This relationship is the consequence of a dimensional analysis, similar to the one arrived at in the previous section for σ. Tissue vicosities η are

Fig. 5. Sorting of chicken embryonic pigmented epithelial cells (dark) from chicken embryonic neural retinal cells (light). The average aggregate size is 200 μm. At the end of sorting, neural retinal cells preferentially wet the external tissue culture medium surrounding the aggregate. (*a*), (*b*), and (*c*) correspond to 17, 42, and 73 h after the initiation of sorting, respectively.

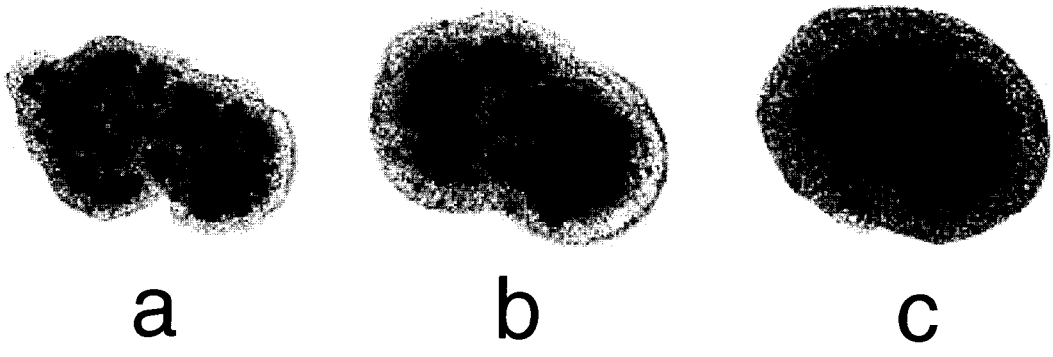

obtained from the friction constant by $\mu \approx d\eta$, where d is the diameter of a cell [36]. The values of η for the five embryonic chicken tissues, derived from μ_2 are all of the order of 10^4–10^5 P [31].

The above analysis shows that once the surface tension and the viscoelastic parameters are determined, one may, in principle, get biologically relevant information on characteristic cell adhesion molecules. In particular, provided the number of such molecules on the cell surface is known, one can determine the effective strength of binding and the lifetime of an adhesion pair. We are currently performing experiments with genetically transformed cells, which express a controlled number of special cell adhesion molecules, i.e., cadherins [37,38] and have no other adhesion mechanism. From these experiments, we hope to gain information on cell adhesion under near physiological conditions.

5. Cell sorting

We have performed sorting experiments with the five embryonic chicken tissues, whose surface tensions and viscoelastic properties had been measured using the parallel-plate compression apparatus [11]. The equilibrium sorting patterns of these tissues were found to be consistent with the measured values of the tensions. Specifically, liver sorts from neural retina ($\sigma_{nr} < \sigma_{liv}$), heart sorts from liver ($\sigma_{liv} < \sigma_h$), pigmented epithelium sorts from heart ($\sigma_h < \sigma_{pe}$), and limb sorts from pigmented epithelium ($\sigma_{pe} < \sigma_l$).

Recently, we have been able to extend the fluid analogy of embryonic tissues to the kinetics of sorting. In Fig. 5, we show snapshots of the cellular pattern at various stages of sorting of pigmented epithelial cells from neural retinal cells. The pattern evolves by the fusion (or coalescence) of domains. The images resemble nucleation in a binary liquid below the critical temperature. In fluids and liquids, interfacial tension between the two phases, σ_1, drives hydrodynamic coalescence, while the viscosity, η_1, of the more viscous phase hinders it [39,40]. When the volume fraction of the minority phase exceeds a critical value ($\phi \sim 0.3$), the pseudo-period L_m, the size of interconnected domains, increases linearly in time, as

$$L_m = b_l(\sigma_l/\eta_l)t \tag{6}$$

Here b_l is a universal constant, independent of material properties [39]. Theory predicts $b_l = 0.04$ [41], in agreement with experiments [42]. Below the critical volume fraction, $L_m \sim t^{1/3}$ [43].

The pseudo-period of the cellular aggregate (with $\phi = 0.27$ for the minority pigmented epithelial cells), shown in Fig. 5 grows linearly in time. Using the interfacial tension σ_{np} ($\sim$10 dyn/cm) between aggregates of neural retinal and pigmented epithelial cells [11] and tissue viscosity determined as

described above, the hydrodynamic expression (6) for L_m leads to $b_t \sim 0.003$ (the cellular analogue of b_l). Given the uncertainties in σ_t (~20%) and η_t (~30%) in these measurements, b_t and b_l agree, supporting the immiscible fluid model of contiguous tissues. Alternatively, assuming the liquid analogy and identifying b_t with b_l, one can estimate σ_{np}, which is not otherwise easy to measure. (The value for σ_{np} we quoted above is $\sigma_{np} = \sigma_{pe} - \sigma_{nr}$, with $\sigma_{pe} = 12.6$ dyn/cm and $\sigma_n = 1.6$ dyn/cm [11]. This estimate uses Young's equation at complete wetting [34], since neural retina wets the interface between pigmented epithelium and the tissue culture medium.) Just as σ_n and σ_{pe} may give information on the cohesiveness of the neural retina and pigmented epithelium, σ_{np} may contain information on the cross adhesion between the cells of the two tissues.

6. Conclusions

In this work, we have demonstrated that various embryonic tissues possess well-defined physical properties characteristic for fluids and viscoelastic materials. A number of morphogenetic processes (e.g., spreading and sorting) can be interpreted in terms of these properties. A physical description of early embryonic phenomena or tissue behavior, however, has merit for biologists only if it leads to specific biological prediction or to any type of biologically useful information. Predictions are usually not easy to make, the simple reason being that the complexity of the biological system does not allow its modeling in terms of a few physical parameters. This may be possible for an inanimate physical system, where simplification and retaining of the "relevant" physics may make sense. It is not clear what is relevant in a biological system. Reducing it, so that its modeling becomes possible, may lead to the complete loss of its biological specificity.

The method of studying living tissues, described in this work, represents a case when biological specificity can be expressed in terms of measurable physical parameters. Moreover, the measured physical parameters can be used to make predictions on vital biological phenomena. One such phenomenon is cell adhesion. Experiments using genetically transformed cells with a controlled number of cadherin-cell adhesion molecules will provide numerical information on the strength of binding between these molecules under near physiological conditions. Below we present an another example of where and how our methods may be used as a diagnostic tool.

An individual suffering from a primary tumor can be saved as long as the tumor does not metastasize [44]. Metastasis and the development of secondary tumors, requires cells to leave the primary tumor and be carried by the circulatory system to a new location. For a cell to dissociate from the primary tumor its adhesion mechanism has to be transformed, its binding to neighbors has to be weakened to a critical point [45]. Thus, the monitoring of changes in the effective strength of adhesion in the tumor may turn out to be critical. Monitoring could be accomplished by the method described in this work. A biopsy of the tumor may provide enough material to form a spherical aggregate of the cancerous cells. This then is subjected to a compression in the parallel plate chamber to measure the surface tension of the tissue to obtain information on the adhesion between its constituent cells. Such experiments, performed at regular time intervals, could indicate when the removal of the primary tumor by surgical means is absolutely necessary to prevent metastasis. Attempts along these lines have already been made by Foty and Steinberg [46,47].

Acknowledgements

This work was supported by research grants from the National Science Foundation under IBN 97-10010 (G.F) and INT 96-03035-06, (J.A.G.), by the Petrloum Research Foundation (J.A.G.) and the Centre National d'Etudes Spatiales (D.B).

References

1. S.A. Newman and W.D. Comper. Development, **110**, 1 (1990).

2. M.S. Steinberg. Integr. Biol. **1**, 49 (1998).
3. P.L. Townes and J. Holtfreter. J. Exp. Zool. **128**, 53 (1955).
4. U. Techau and T.W. Holstein. Dev. Biol. **151**, 117, (1992).
5. M.S. Steinberg and M. Takeichi. Proc. Natl. Acad. Sci. U.S.A. **91**, 206 (1994).
6. M.S. Steinberg. Science (Washington), **141**, 401 (1963).
7. M.S. Steinberg. *In* Cellular membranes in development. *Edited by* M. Locke. Academic Press, New York. 1964. p. 321.
8. M.S. Steinberg. J. Exp. Zool. **173**, 395 (1970).
9. M.S. Steinberg. *In* Dynamical phenomena at interfaces, surfaces and membranes. *Edited by* D. Beysens, N. Boccara, and G. Forgacs. Nova Science Publishers, Commack, New York. 1993. p. 3.
10. M.S. Steinberg and T.J. Poole. *In* Cell behaviour. *Edited by* R. Bellairs, A.S.G. Curtis, and G. Dunn. Cambridge University Press, Cambridge. 1982. p. 583.
11. R.A. Foty, C.M. Pfleger, G. Forgacs, and M.S. Steinberg. Development, **122**, 1611 (1996).
12. J.A. Glazier and F. Graner. Phys. Rev. E: Stat. Phys. Plasmas Fluids Relat. Interdiscip. Top. **47**, 2128 (1993).
13. J.C.M. Mombach, J.A. Glazier, R.C. Raphael, and M. Zajac. Phys. Rev. Lett. **75**, 2244 (1995).
14. D. Godt and U. Tepass. Nature (London), **395**, 387 (1998).
15. A. González-Reyes and D. St. Johnston. Development, **125**, 2837 (1998).
16. H.M. Phillips and M.S. Steinberg. J. Cell Sci. **30**, 1 (1978).
17. H.M. Phillips, M.S. Steinberg, and B.H. Lipton. Dev. Biol. **59**, 124 (1977).
18. Y. Hiramoto. J. Cell Physiol. **69**, 219 (1968).
19. Y. Hiramoto. Exp. Cell Res. **56**, 201 (1960).
20. P.A. Valberg and D.F. Albertini. J. Cell Biol. **101**, 130 (1985).
21. T.Y. Sakanishi. Biorheology, **25**, 123 (1988).
22. R.M. Hochmuth, H.P. Ting-Beal, B.B. Beaty, D. Needham, and R. Tran-Son-Tay. Biophys. J. **64**, 1596 (1993).
23. G.K. Ragsdale, J. Phelps, and K. Luby-Phelps. Biophys. J. **73**, 2798 (1997).
24. K.S. Zaner and P.A. Valberg. J. Cell. Biol. **109**, 2233 (1989).
25. O. Müller, H.E. Gaub, M. Bärmann, and E. Sackmann. Macromolecules, **24**, 3111 (1991).
26. P.A. Janmey. Curr. Opin. Cell Biol. **2**, 4 (1991).
27. M. Tempel, G. Isenberg, and E. Sackmann. Phys. Rev. E: Stat. Phys. Plasmas Fluids Relat. Interdiscip. Top. **54**, 1802 (1996).
28. H. Engelhardt and E. Sackmann. Biophys. J. **54**, 495 (1988).
29. Y.C. Fung. Biomechanics. Springer-Verlag, New York. 1993.
30. R. Gordon, N.S. Goel, M.S. Steinberg, and L.L. Wiseman. J. Theor. Biol. **37**, 43 (1972).
31. G. Forgacs, R.A. Foty, Y. Shafrir, and M.S. Steinberg. Biophys. J. **74**, 2227 (1998).
32. P.B. Armstrong. Crit. Rev. Biochem. Mol. Biol. **24**, 119 (1989).
33. A. Folkman and A. Moscona. Nature (London), **273**, 345 (1978).
34. J.S. Rowlinson and B. Widom. Molecular theory of capillarity. Clarendon Press, Oxford. 1989.
35. H.M. Phillips and G.S. Davis. Am. Zool. **18**, 81 (1978).
36. A.R. Bausch, F. Ziemann, A.A. Boulbitch, K. Jacobson, and E. Sackmann. Biophys. J. **75**, 2038 (1998).
37. M. Takeichi. Science (Washington), **251**, 1451 (1991).
38. B.M. Gumbiner. Cell, **84**, 345 (1996).
39. E. Siggia. Phys. Rev. A: Gen. Phys. **20**, 595 (1979).
40. A. Onuki. Europhys. Lett. **28**, 175 (1994).
41. V.S. Nikolayev, D. Beysens, and P. Guenoun. Phys. Rev. Lett. **76**, 3144 (1996).
42. P. Guenoun, R. Gastaud, F. Perrot, and D. Beysens. Phys. Rev. A: Gen. Phys. **36**, 4876 (1987).
43. D. Beysens. Physica A, **239**, 329, (1997).
44. A. Ahmad and I.R. Hart. Crit. Rev. Oncol. Hematol. **26**, 163 (1997).
45. J. Behrens, M.M. Mareel, F.M. Van Roy, and W. Birchmeier. J. Cell Biol. **108**, 2435 (1989).
46. R.A. Foty and M.S. Steinberg. Cancer Res. **57**, 5033 (1997).
47. M.S. Steinberg and R.A. Foty. J. Cell Physiol. **173**, 135 (1997).